Ground-level ozone in Mekong delta region: precursors, meteorological factors, and regional transport

Long Ta Bui (longbt62@hcmut.edu.vn)

Ho Chi Minh City University of Technology: Truong Dai hoc Bach khoa Dai hoc Quoc gia Thanh pho Ho Chi Minh https://orcid.org/0000-0003-1884-8520

Phong Hoang Nguyen

Ho Chi Minh City University of Technology

Research Article

Keywords: Mekong delta, Ozone, Emission precursors, Meteorological factors, WRF/CMAQ

Posted Date: May 12th, 2022

DOI: https://doi.org/10.21203/rs.3.rs-1520119/v1

Abstract

The Mekong Delta region (MDR), also known as Vietnam's rice bowl, produced a bountiful harvest of about 23.8 million tons in 2020, accounting for 55.7% of the country's total production, providing food security for 20% of the world population. With the rapid pace of industrialisation and urbanisation, concentration of ozone in the lower atmosphere has risen to a level that reduces crop yields, especially rice, and is, therefore, the subject of research. This study has a goals to simulate the spatio–temporal distribution of ground-level ozone in the area, also to evaluate the impact of precursor emissions and meteorological factors on spatio–temporal distributions of concentration. The study area was divided into six agro-ecological zones to clarify the role of emissions in each zone. The simulation results showed that the ground-level O_3 in the MDR ranged from 40.39 μg/m^3 to 52.13 μg/m^3. In six agro-ecological zones, the average annual ground-level O_3 concentration was relatively high, and was the highest in areas six (CZ) and seven (CPZ), with 46.11 μg/m^3 and 46.41 μg/m^3, respectively. In each zone, the annual average O_3 concentration tended to gradually increase from the inner delta to coastal areas. Two types of precursors, NO_x and NMVOCs, are the main contributors to O_3 pollution, with the largest contribution coming from zone 1 (FAZ) with 91.5 thousand tons of NO_x/year and 455.2 thousand tons of NMVOCs/year. Among the meteorological factors considered, relative humidity (RH) and surface pressure (P) were the two main factors that contributed to the increase in ground-level ozone. The spatio–temporal distribution of ground-level O_3 in the MDR was influenced by emission precursors from different zones as well as meteorological factors. The present results can help policymakers formulate plans for agro-industrial development in the entire region.

1 Introduction

Although, ground-level ozone is essential in the Earth's upper atmosphere, its presence in the lower atmosphere acts as a secondary air pollutant which negatively impacts human health and crops (Wilkinson et al., 2012). The effect of phytotoxic ozone concentrations on crop yields has been extensively studied (Pleijel, 2011; Arshad, 2021; Ramya et al., 2021; Wang et al., 2021; Shang et al., 2022). Europe's economic loss in 2000 was estimated at €6.7 billion, based on the effects of ground-level ozone on 23 crops, (Ene et al., 2015); losses in global crop production for the same year were estimated at $11–18 billion USD (Avnery et al., 2011). Recent studies have shown that rice crops are also sensitive to ground-level O_3, especially in Asian cultivars (Shang et al., 2022). Several pilot studies conducted in Malaysia, Pakistan, and Vietnam have shown that the local rice varieties are affected by O_3 (Ishii et al., 2007; Arshad, 2021)

Ground-level ozone has long been recognized as a threat to crop health and human health, and studies on its effects have been conducted (Nouchi et al., 1991; Wahid et al., 1995; Brunekreef et al., 2002; Tang et al., 2014;). Plants that grow under favourable conditions form stomata on leaf surfaces to exchange gases for photosynthesis (Emberson et al., 2009). In this case, ozone is one of the gases that can penetrate plants. The reduction in crop yields due to the cumulative effects of ground-level ozone is

evident when ozone “waves” are prolonged; if this period coincides with a significant increase in precursor emissions, the effect is doubled (Feng et al., 2009). Symptoms of injury can be observed through leaf wilt or necrosis on the leaf surface, which can coalesce to form larger areas of injury; the leaves often dry up and fall prematurely (Emberson et al., 2009). Ozone reduces grain size, weight, nutritional quality in field crops such as certain varieties of wheat, rice, maize, beans, and soybeans (Biswas et al., 2008; Decock et al., 2012)

Asian rice (*Oryza sativa*) is an important food crop, supplying more than half of the world's population, particularly in Asia and Africa (Doliente et al., 2021). The impact of ground-level ozone on local rice varieties in Asia may be of greater interest, given the important role played by agriculture in this region (Chen et al., 2008). Recent studies have shown that rice is sensitive to ground-level ozone, especially in Asian cultivars (Olszyk et al., 1997; Tang et al., 2014; Shang et al., 2022). Several pilot studies conducted in Malaysia, Pakistan, and Vietnam have shown that local rice varieties are affected by ground-level ozone (Wahid et al., 1995; Ishii et al., 2007). Therefore, it is important to assess the extent and scope of rice production loss due to ground-level ozone exposure, particularly in Southeast Asia, home to the world's two largest rice exporters, Thailand and Vietnam (Emberson et al., 2009). Even though people worldwide depend on rice grown in the MDR, there are few quantitative studies on ground-level ozone distribution (Ishii et al., 2004, 2007; Cha-um et al., 2007; Chen et al., 2008;Yamaguchi et al., 2014).

The Mekong Delta region (MDR) of Vietnam has an area of nearly 40,000 km^2 and a population of nearly 18 million, accounting for approximately 12% of the land area and 22% of the country's population. This is a land with a strategic location in Vietnam, bordering the East Sea and Southwest Sea on three sides, with a coastline of more than 700 km with 360,000 km^2, and an exclusive economic zone in a strategic location that is very favourable for economic development (Nguyen et al., 2019; Tran et al., 2019). The MDR, also known as the "rice bowl" of Vietnam, produced a bountiful yield of around 23.8 million tons in 2020, accounting for 55.7% of the country's total yields (Wassmann et al., 2019; Tu et al., 2021; Bich et al., 2022; Ferrer et al., 2022), providing food security for 20% of the world's population, particularly in regions where rice is the staple diet. With accelerated industrialization and urbanization of the MDR's, the concentration of ground-level ozone in the lower atmosphere has risen to levels that have resulted in reduced agricultural yields, particularly of rice; it is therefore the focus of this research (Danh et al., 2016).

Ground-level ozone is produced by nitrogen oxides (NO_x) and volatile organic compounds (VOCs) through photochemical reactions (Emberson et al., 2009; Guo et al., 2019); therefore ground-level ozone dispersion was simulated through the application of photochemical transport and meteorological models (Hogrefe et al., 2000; Sokhi et al., 2006; Davis et al., 2011; Li et al., 2014; Wang et al., 2015; Astitha et al., 2017; Trieu et al., 2017; Wang et al., 2017; Chen et al., 2021; Mousavinezhad et al., 2021; Wang et al., 2021). The using meteorological/ photochemical transport models to predict hourly ground-level ozone concentrations, and the modelling results were evaluated based on the measured field data were done in a various studies (Sokhi et al., 2006; Davis et al., 2011; Li et al., 2014; Wang et al., 2015).

Ground-level ozone concentrations often occur on days with strong sunlight and weak winds, creating favourable conditions for the production and accumulation of ozone and its precursors (Wang et al., 2017). Wind direction was also important because it affects the transport of pollution, thereby increasing the temperature of windy sites (Epa, 2006; Li et al., 2014; Mitchell et al., 2021). The quantification of ozone production from different precursors, including NO_X, VOCs, and individual VOC species, was performed (Garner et al., 2013; Simon et al., 2015; Wang et al., 2015). Thus, with the help of these models, it was possible to propose solutions to reduce ozone pollution by minimising precursor emissions (Xue et al., 2014; Wang et al., 2017).

Favourable meteorological conditions for photochemical episodes have been extensively studied (Camalier et al., 2007; Simon et al., 2012; McNider et al., 2020). For example, sunny weather and low wind velocity lead to pollution accumulation and O_3 production (Xue et al., 2014; Carter et al., 2017). Several studies have been conducted to determine the relationship between ozone concentration and local meteorological parameters, including solar irradiance, temperature, relative humidity, wind speed and direction, and cloud cover (Wang et al., 2017).

Given the special importance of the Mekong Delta to world food security, this study was conducted with the goal of applying WRF/CMAQ in combination with MLR models, on the one hand simulating the spatio–temporal distribution of ground-level ozone in the region, and on the other hand evaluating the impact of precursor emissions and meteorological factors on the spatio–temporal distribution variation of ground-level ozone. The results allow the formulation of long-term and medium-term plans for socio-economic development, coupled with environmental protection, with attention to costs, economic benefits, and environmental efficiency.

2 Data And Method

2.1 Study area

The Mekong Delta Region (MDR) consists of 13 provinces (Fig. 1). According to data from the General Statistics Office of Vietnam in 2019, the Mekong River Delta has the largest total area in Vietnam, with a higher economic growth rate than the whole country. Rice farms alone account for 47% of the area and 56% of the country's rice production, and rice exports from the entire region account for 90% of production (GSO, 2020; Cramb, 2020).

Based on geographical, agricultural, water resource features, the MDR can be classified into six agro-ecological zones, excluding hills and mountains (Nguyen et al., 2007). These areas are affected by flooding or saline intrusion, as indicated by the demarcation lines in Fig. 1 (Nguyen et al., 2007). These six zones include the freshwater alluvial zone (FAZ), which is located along the Trans-Bassac and Mekong rivers in the central part of the delta, and is characterised by alluvial soils, covering an area of approximately 900,000 ha of available fresh water. In this zone, people make a living by diversifying agricultural activities, practising two- or three-crop rice farming combined with the cultivation of fruit

trees, vegetables, and aquaculture. Next is the Dong Thap Muoi zone (PRZ), located in Dong Thap province and part of Long An province, with an area of approximately 500,000 ha. This is the upper part of the delta with 0.5 m lower than average sea level. The area had alkaline soil, and water and related environmental factors were partially controlled by flooding and acid toxicity. People in this area make a living with rice farming and integrated aquaculture. The third zone is the Long Xuyen-Ha Tien Quadrangle (LXZ), located between the two provinces of An Giang and Kien Giang, with an area of 400,000 ha, and is also characterised by alkaline soil. Water and environmental factors changed from salty alum ecology to freshwater ecology after 2000. Rice is the main crop in the area, and rice-based farming is the main activity. The fourth area is the Trans-Bassac Depression Zone (TBZ), located to the west of Can Tho, covering an area of approximately 600,000 ha. This is a low-lying area on a plain that is not seriously affected by floods and saline intrusion and has favourable conditions for intensive farming and diverse crop production. Residents make a living by cultivating two or three rice crops. The coastal zone (CZ), located along the eastern part of the Mekong Delta, covers approximately 600,000 ha. Large areas in this zone have acidic soil. Since 1998, parts of this region have been subject to changing water and environmental conditions from brackish to permanent freshwater ecology. In this area, people earn a living by farming shrimp and growing rice. The Ca Mau Peninsula (CPZ), located at the southernmost tip of the delta, covers an area of approximately 800,000 ha. The area is characterised by seasonal salinisation of the soil and various rice-based farming systems in terms of rainwater use. Since 1998, large swaths of the region have undergone changes in water and environmental conditions to a permanent freshwater eco-environment, with shrimp farming being the dominant activity here (Nguyen et al., 2007).

Figure 1. *Study area*

2.2 Data

2.2.1 Meteorology

In this study, the hourly realistic meteorological data from the observation stations of Can Tho and Tien Giang (Fig. 2) in the freshwater alluvial area and Kien Giang in the lowland area were extracted in March and October 2018 representing the dry and wet seasons of the MDR from the websites of https://www.wunderground.com/ and https://www.timeanddate.com/, respectively. A time-series dataset of temperature, wind speed, wind direction, relative humidity, and surface pressure was captured from each monitoring site, which was used to verify the results of the WRF simulations in terms of accuracy and error levels using statistical indicators.

Figure 2. The measuring sites of ground-level O_3 and meteorological parameters

2.2.2 Observation of ground-level O_3

In 2018, the field-measured ground-level O_3 concentration datasets were obtained from 11 monitoring sites, including N, NT1, DT1, DT3, DT4, DT6, GT2, GT3, CN1, CN2, and CN4 (Fig. 2), which had been managed and operated by the Binh Duong Center of Natural Resources and Environment-Technical Monitoring (BREM) (Binh Duong, 2019). These datasets were used to support the processes of calibration and validation of the ground-level O_3 concentration results simulated by the coupled WRF/CMAQ model. In addition, ground-level O_3 concentration datasets were obtained by manual and discontinuity measurements four times during the monitoring days (Fig. 2).

2.2.3 Emission inventory datasets

In this study, the usage emissions dataset named CAMS-GLOB-ANT was provided by Emissions of Atmospheric Compounds and Compilation of Ancillary Data (ECCAD) (https://eccad3.sedoo.fr/), developed by the Copernicus Atmosphere Monitoring Service, and published in 2018 (ECCAD, 2020; Granier et al., 2019). This is an output product from a combination of EDGARv4.3.2 emission data built by the Common European (Crippa et al., 2018) and the Community Emissions Data System (CEDS) emission inventory (Hoesly et al., 2018) providing emissions data for the next IPCC report, AR6.

The CAMS-GLOB-ANT dataset is a global emissions inventory dataset from a variety of sectors and is available for the period 2000–2020. Because the sectors contributing to the emissions of EDGAR v4.3.2 and CEDS are heterogeneous, the Copernicus Atmosphere Monitoring Service defines general global emission activity groups for the CAMS-GLOB-ANT dataset to ensure a match between the two data sources (Granier et al., 2019). The global emission flux of different substances in the CAMS-GLOB-ANT dataset was estimated from 14 sectors of anthropogenic emissions, including power generation[1] (ENE), road transportation[2] (TRO), off-road transportation[3] (TNR), fugitives[4] (FEF), industrial process[5] (IND), solvents[6] (SLV), ships[7] (SHP), solid waste and wastewater[8] (SWD), residential and other sectors[9] (RES), agriculture livestock[10] (AGL), agriculture soils[11] (AGS), agricultural waste burning[12] (AWB), general agriculture activities[13] (AGR), and total contribution of sectors[14] (SUM) (Granier et al., 2019).

The used dataset of inventory and emission load estimation, including 19 primary substances (EC, OC, PMC, PMOTHR, PNCOM, H_2O, K^+, Na^+, Ca^{2+}, Al^{3+}, $Fe^{2+/3+}$, Mg^{2+}, Mn^{2+}, Si^{4+}, Ti^{2+}, NH_4^+, Cl^-, NO_3^-, and và SO_4^{2-}) and 34 substances joining in secondary reactions (NO_x, SO_2, NH_3, CO, CO_2, CH_4, BC, OC, NMVOCs, and 25 other VOCs species) contribute to ground O_3 formation encoded according to the Carbon Bond 05 chemical mechanism (Sarwar et al., 2008). The inventory emission dataset was generated by monthly averages with a spatial resolution of $0.1^o \times 0.1^o$ (Granier et al., 2019). Emissions of different VOC species were also available in the global emission dataset of CAMS-GLOB-ANT according to each VOC-contributing sector (Granier et al., 2019). In this study, the CAMS-GLOB-ANT global dataset, version V2.1 created for the 2000–2020 period, (Granier et al., 2019) was used to analyse anthropogenic emission contributions in the Mekong Delta region. The results of emission data processing are shown in the Fig. S1 – S36.

2.3 WRF/CMAQ

2.3.1 Nested domain setup in the coupled WRF/CMAQ

The model of WRF (Weather Research and Forecasting) with version 3.8 (Skamarock et al., 2008) combined with the Community Multiscale Air Quality Modelling System (CMAQ) ver. 5.2.1 were used by Borge et al. (2014), Hu et al. (2015), and Lang et al. (2017) to simulate ground-level ozone (O_3) in Southern Vietnam between 01 January, 2018, and 31 December, 2018.

Two level nested simulation calculation domains, D01 and D02, were set up in the WRF/CMAQ coupled models, where computational domain D01 had spatial resolution of approximately ~ 30.43 km × 30.43 km, and was the largest domain (76 columns and 94 rows; the area of D01 was approximately 5.41 × 106 km^2). Domain D02 had a spatial resolution of approximately 9.55 km × 9.55 km was the second domain nested in the D01 domain (55 columns and 43 rows; the area of the D02 domain was about ~ 2.11 × 105 km^2). The details of the specifications of calculation domains D01 and D02 are shown in Table 1. Domain D01 covers all of Vietnam, while D02 consists of most of the southern provinces, including the Mekong Delta provinces (or the study area), the Southeast, and part of the South Central and Central highlands provinces, which might have the most significant influence on the research area. The boundary conditions of D02 were determined according to D01. The boundary conditions of the largest domain, D01 were provided by the default configuration available in the CMAQ software. The hourly meteorological fields according to the input requirements of the CMAQ model were simulated by a WRF model using data from the National Center for Environmental Prediction (NCEP) Final (FNL) Operational Global Analysis (https://rda.ucar.edu/datasets/ds083.2/) (NCEP, 2000) and were considered as the original meteorological conditions and boundary meteorological conditions for the coupled model.

Table 1
Setup of the computing spatial domains for ground-level O_3 simulations by the coupled WRF/CMAQ models

Domain parameters	Domain D01	Domain D02
Domain range	Vietnam	Southern provinces of Vietnam (Study area)
Grid size, X [km] × Y [km]	2,312.68 × 2,860.42	525.25 × 410.65
Số nút lưới tính, $N_x \times N_y$	75 × 93	54 × 42
Total numer of grid size	7,144	2,365
Grid size (km)	30.43	9.55
Center coordinate	(13.3826^o; 104.969^o)	(10.1195^o; 105.955^o)
Coordinate system	Asia Lambert Conformal Conic	Asia Lambert Conformal Conic
Setup domain type	The nested modelling domain	The nested modelling domain

Table 1. Setup of the computing spatial domains for ground-level O_3 simulations by the coupled WRF/CMAQ model

2.3. 2 WRF/CMAQ modelling performance evaluation

In this study, the fusion data method between the measured and simulated ground-level O_3 results was used to correct the initial outcomes estimated by the coupled WRF/CMAQ model based on the study outcomes of Friberg et al., (2016) and Senthilkumar et al., (2019). Eq. (1) illustrates the calculation of two regression parameters, α and β, reflecting the correlation relationship applied to correct the computed ground-level O_3 concentration results by the coupled WRF/CMAQ model as follows:

$$CMAQ_{x,\,Corrected} = \alpha CMAQ_x^{\beta} \quad (1)$$

where $CMAQ_x$ is the exported initial ground-level O_3 concentration based on the computing results of the coupled WRF/CMAQ model at the observing stations *x* of the given time *t* (h); $CMAQ_{x,\,Corrected}$ is the verified ground-level O_3 concentration close to the field measured data in the monitoring sites *x* of the specific time *t* (h), and α and β are the coefficients of the correlation equation used for calibration.

The outcomes of the calculated ground-level O_3 concentration by WRF/CMAQ after using the corrected functional equation were verified according to the measured O_3 concentration at the observation stations

in Binh Duong Province. Based on statistical indexes for evaluating the simulation capabilities of the coupled WRF/CMAQ model, which includes the coefficients of the Nash-Sutcliffe Efficiency (NSE) (2), other statistical indices such as the mean bias (MB) (3), root mean squared error (RMSE) (4), normalised mean bias (NMB) (5), normalised mean gross Error (NME) (6), and the correlation coefficient *R* (7) were estimated as follows (Wang et al., 2021):

$$NSE(Nash) = 1 - \frac{\sum_{1}^{N}(M_i - O_i)^2}{\sum_{1}^{N}(O_i - \bar{O}_i)^2}$$

2

$$MB = \frac{1}{N}\sum_{i=1}^{N}(M_i - O_i)$$

3

$$RMSE = \sqrt{\frac{1}{N}\sum_{1}^{N}(M_i - O_i)^2}$$

4

$$NMB = \frac{\sum_{1}^{N}(M_i - O_i)}{\sum_{1}^{N}(O_i)} \times 100$$

5

$$NME = \frac{\sum_{1}^{N}\left|M_i - O_i\right|}{\sum_{1}^{N}(O_i)} \times 100$$

6

$$R = \frac{\sum_{i=1}^{N}\left[(M_i - \bar{M}_i) \times (O_i - \bar{O}_i)\right]}{\sqrt{\sum_{i=1}^{N}(M_i - \bar{O}_i)^2} \times \sqrt{\sum_{i=1}^{N}(O_i - \bar{O}_i)^2}}$$

7

where $\bar{M_i}$ is the result of the ground-level O_3 concentration simulated by the combined WRF/CMAQ models, M_i is the average ground-level O_3 software simulation result, O_i is the result of ground-level O_3 concentrations from five measuring stations in the districts of Binh Duong Province (in domain D02), $\bar{O_i}$ is the average ground-level O_3 result from the monitoring stations in the study area, and *N* is the size of the validated sample.

Calibration equations 9 and 19 were built according to (1) from the simulated results extracted at the ground-level O_3 measuring stations (Fig. 2). Coefficients α and β were determined based on the difference between the actual measured and modelled datasets.

Accuracy verifications of the estimated results using the coupled WRF/CMAQ model based on statistical indicators (2)–(7) and Table 2. The NSE values in the three field-measured sites of CN1, NT1, and CN4 were NSE_{CN1}=0.918, NSE_{NT1}=0.987, and NSE_{CN4}=0.928, respectively, reaching a good level; however, the values of station DT1 achieved a good level with NSE_{DT1} = 0.888 (with NSE > 0.800), and station GT2 also had a slightly good level with NSE_{GT2} = 0.729 (with NSE > 0.700). Furthermore, other statistical indexes also showed that the simulation capability of the coupled WRF/CMAQ model was from a good level to an excellent level. Specifically, the RMSE and MB indices of measuring station DT1 were 4.648 and 0.537, respectively; those of observation station GT2 were 23.330 and − 0.540, respectively; those of monitoring sites CN1 were 3.943 and 0.127, respectively; those of measuring station NT1 were 1.891 and 0.464, respectively; those of monitoring site CN4 were 4.419 and − 0.091, respectively. Similarly, other indices consisting of NMB, NME, and the calculated correlation coefficient *R* in the above 5 measuring stations all met the given allowable conditions; specifically, these values of the measuring sites were respectively as follows: NMB_{DT1}=2.254%; NMB_{GT2}=-0.669%; NMB_{CN1}=0.568%; NMB_{NT1}=0.267%; NMB_{CN4}=-0.362% (with the criteria of -30% <NMB < 30%); NME_{DT1}=13.060%; NME_{GT2}=13.440%; NME_{CN1}=12.635%; NME_{NT1}=6.998%; and NME_{CN4}=10.697% (with the criteria of NME < 50%) and the correlation coefficients of R_{DT1}=0.944; R_{GT2}=0.856; R_{CN1}=0.959; R_{NT1}=0.995, and R_{CN4}=0.963 (with the criteria of R > 0.5) (Table 2). The simulated ground-level O_3 concentration calibration equations established for each month of 2018 are shown in Table 3.

Table 2
Recommended benchmarks for ground-level O_3 concentration modelling by the coupled WRF/CMAQ model in this study

The statistical indexes	Range of value	Benchmarks	References
NSE (Nash)	(-∞; +1]	0.40–0.65: (GSO, 2020)Pass 0.65–0.85: Good > 0.85: Excellent	(McCuen et al., 2006; Xiaohui Zhong et al., 2015; Knoben et al., 2019)
MB (Mean Bias)	(-∞; +∞)	-	(Morris et al., 2005; Eder et al. 2006; Emery et al., 2017; Nguyen et al., 2020)
RMSE (Root Mean Squared Error)	(-∞; +∞)	-	(Morris et al., 2005; Eder et al., 2006; Emery et al., 2017; Nguyen et al., 2020)
NMB (Normalised Mean Bias)	(-100%; +∞)	-30% < NMB < + 30%	(Morris et al., 2005; Eder et al., 2006; Emery et al., 2017; Nguyen et al., 2020),
NME (Normalised Mean Gross Error)	(0%; +∞)	< 50%	(Morris et al., 2005; Eder et al. 2006; Emery et al., 2017; Nguyen et al., 2020)
Correlation coefficient *R*	[-1; +1]	*R* < 0.40: Not pass 0.40 < *R* < 0.80: Pass 0.80 < *R* < 0.85: Good *R* > 0.85: Excellent	(Emery et al., 2017; Nguyen et al., 2020)

Table 3
Equation to calibration ground - level O3 concentration by month, 2018

Month	Calibrated equations for ground- level ozone concentration O_3	Month	Calibrated equations for ground- level ozone concentration O_3
1	$y = 1.0332\ x^{0.9814}$ ($R^2 = 0.9844$) (8) α= 1.0332 and β = 0.9814 (0 < β < 1)	7	$y = 1.07227\ x^{0.9758}$ ($R^2 = 0.9976$) (14) α = 1.07227 and β = 0.9758 (0 < β < 1)
2	$y = 0.9666\ x^{0.9924}$ ($R^2 = 0.9983$) (9) α = 0.9666 and β = 0.9924 (0 < β < 1)	8	$y = 1.0156\ x^{0.9882}$ ($R^2 = 0.9938$) (15) α = 1.0156 and β = 0.9882 (0 < β < 1)
3	$y = 1.0985\ x^{0.9742}$ ($R^2 = 0.9641$) (10) α = 1.0985 and β = 0.9742 (0 < β < 1)	9	$y = 0.9845x^{0.9961}$ ($R^2 = 0.9886$) (16) α = 0.9845 and β = 0.9961 (0 < β < 1)
4	$y = 1.0985\ x^{0.9742}$ ($R^2 = 0.9943$) (11) α = 1.0985 and β = 0.9742 (0 < β < 1)	10	$y = 1.0473\ x^{0.9855}$ ($R^2 = 0.9317$) (17) α = 1.0473 and β = 0.9855 (0 < β < 1)
5	$y = 0.9589\ x^{0.9882}$ ($R^2 = 0.9714$) (12) α = 0.9589 and β = 0.9882 (0 < β < 1)	11	$y = 0.9437x^{0.9975}$ ($R^2 = 0.9969$) (18) α = 0.9437 and β = 0.9975 (0 < β < 1)
6	$y = 1.0799\ x^{0.9895}$ ($R^2 = 0.9937$) (13) α = 1.0799 and β = 0.9895 (0 < β < 1)	12	$y = 1.0745\ x^{0.9891}$ ($R^2 = 0.9851$) (19) α = 1.0745 and β = 0.9891 (0 < β < 1)

Table 2. Recommended benchmarks for applying ground-level O3 concentration modelling by the coupled WRF/CMAQ model

Table 3. Equation to calibration ground - level O3 concentration by month, 2018

2.4 Multiple linear regression

Multiple linear regressions (MLR) (Amos P.K. Tai et al., 2010, 2012) were established to clarify the multiple linear correlations of the ground-level O_3 concentration with meteorological variables (i), precursor emission variables (ii) and both types of the above-mentioned variables (iii). The hourly and daily average ground-level O_3 concentrations correspond to meteorological data and precursor emissions, respectively. Detailed MLR models were built in the form of Eq. 20, as follows:

$$y_{i,j} = \alpha + \beta_1 x_1 + \beta_2 x_2 + \ldots + \beta_{k-1} x_{k-1} + \beta_k x_k + \varepsilon$$

20

where a is the cut-off point on the vertical axis, β, β_1, β_2,..., β_{k-1} and β_k are the slopes or regression coefficients (parameters), and ε is a random variable (an error term). First, the (**20)** was considered for three cases, in which case (i) presents the relationship between the ground-level O_3 concentration (C_{O3}) and three meteorological factors: temperature x_1 (T), relative humidity of x_2 (RH), and surface pressure (referred to as pressure) x_3 (P); in other words, it was crucial to generate a correlation function of C_{O3} = F (T, RH, and P). The next case (ii) considered the correlations between ground-level O_3 concentration (C_{O3}) and five types of precursor emissions, specifically, the CH_4 emission factor was E_{CH4}, x_1; the CO emission factor was E_{CO}, x_2; the NO_x emission factor was E_{NOx}, x_3; the NMVOCs emission factor was E_{NMVOCs}, x_4; other VOCs emission factors were $E_{Other-VOCs}$, x_5, or C_{O3}=F (E_{CH4}, $E_{CO,}$ E_{NOx}, E_{NMVOCs}, and $E_{Other-VOCs}$) for six zones of the MDR (corresponding to six agro-ecological zones). Finally, case (iii) obtained the correlation of C_{O3}=F (T, RH, P, E_{CH4}, $E_{CO,}$ E_{NOx}, E_{NMVOCs}, and $E_{Other-VOCs}$). The obtained fundamental results were linear regression equations showing the multivariable correlation between ground-level O_3 concentration and meteorological variables (x_1, x_2, x_3) and precursor emissions (x_4, x_5, x_6, x_7, x_8). MLR models were created for six zones of the MDR, namely FAZ, PRZ, LXZ, TBZ, CZ, and CPZ (except for zone four, which was HMZ). For cases (i), (ii), and (iii), the k values were 3, 5, and 8, respectively; j is the correspondence for each area according to the zoning in the MDR (j corresponds to the agro-ecological zones, i = one to three, and five to seven; excluding i = four (for which we did not estimate emission values because of the hill and mountainous areas); i = 1 to 3 for cases (i), (ii), and (iii).

2.5 Meteorological modelling

During the dry season, the wind direction at all three meteorological observation sites followed the same patterns in Can Tho, Kien Giang, and Tien Giang (Fig. 2); The dominant direction of the wind was southeast, and the wind speed ranged from 3.3 m/s to 5.5 m/s (considered a light breeze). In the wet season, the wind speed ranged between 5.5 m/s and 7.9 m/s (considered a moderate breeze), and the dominant direction of the wind was also southwest. Furthermore, in the wet season at the two measuring stations in Kien Giang and Tien Giang, the northeast wind direction was observed with a high frequency and the wind speed ranged from 3.3 m/s to 5.5 m/s (considered as the light breeze level).

The simulated meteorological parameter results also showed that the relative humidity in the wet season was higher than that in the dry season at all times. At the Can Tho station, the relative humidity in the dry season was approximately 68.3%, whereas in the wet season, this value increased by 15.0%, reaching approximately 83.5%. Among the three measuring stations, the Can Tho station observed a larger difference than the other two stations; the humidity difference of the Can Tho, Kien Giang, and Tien Giang stations obtained was 15.2%, 12.9%, and 12.4%, respectively. In contrast to the relative humidity factor, the surface pressure during the wet season was higher during the wet season, but the difference was not high, ranging from 0.2 to 0.3 mbar. The monthly mean surface pressure in both seasons showed a declining trend at the measuring stations of Can Tho, Kien Giang, and Tien Giang (Fig. 2).

The WRF simulation was validated based on the field-measured outcomes, as shown in Table S1. The meteorological parameters of temperature, wind speed, wind direction, relative humidity, and surface pressure were used for the evaluation processes. In particular, the statistical indicators showed that the simulated pressure factor had high accuracy, with an RMSE value between 1.28 and 2.00. The Tien Giang station observed the values of wind speed (in both seasons) and wind direction in the dry season with errors within an allowable limit. The RMSE index values of the wind speed factor at these stations were 1.6 and 1.7, respectively, for the dry and wet seasons. The MB index value of the wind speed factor in the wet season was 0.11, and the wind direction factor in the dry season was approximately 5.18. The temperature parameter obtained an acceptable error level with the RMSE index values ranged from 2.19 to 2.80, whereas the values of the relative humidity parameter had an average error level, ranging from 9.05 to 16.38. Among the five considered meteorological parameters, the wind direction parameter estimated a relatively high error level than the other parameters, with the RMSE index value ranging between 74.54 and 159.15.

The estimated meteorological factor results consisting of the temperature, relative humidity, and surface pressure used to assess the study area were also applied in the CMAQ model shown in Figures S37–S39.

2.6 Implementation steps

The Information/data-model system and processing steps used in this study are shown in Figure 3. The steps for processing the emission data are described in Section 2.2.3. The steps of processing the results and creating a meteorological dataset using the WRF model are described in Section 2.3.1. The field measured data of the meteorological and ozone measurements are shown in Sections 2.2.1 and 2.2.2. The steps for calibrating and validating the CMAQ model are presented in Section 2.3. The MLR model determined the relationship between O_3 concentration, emissions, and meteorology, as shown in Section 2.4. To evaluate the accuracy of the meteorological simulation results are presented in Section 2.5, the concentration simulation are presented in Section 2.3.

Figure 3. Implementation steps

3 Result

3.1 Spatio - temporal distributions of ground-level ozone concentration

The simulation results over the entire MDR showed that the ground-level ozone concentration in the region ranges from 40.39 $\mu g/m^3$ to 52.13 $\mu g/m^3$. In zone one (FAZ), O_3 concentrations ranged from 40.45 $\mu g/m^3$ to 49.63 $\mu g/m^3$; in zone two (PRZ) this value ranges from 40.39–43.11 $\mu g/m^3$; in zone three (LXZ) in the range 42.13–48.01 $\mu g/m^3$; in zone four (HMZ) the concentration ranged from 42.39 $\mu g/m^3$ to 44.77 $\mu g/m^3$; in zone five (TBZ) between 41.42–47.02 $\mu g/m^3$; in zone six (CZ) the concentration

ranged from 42.65 μg/m^3 to 50.22 μg/m^3; in zone seven (CPZ) this value ranged from 42.85 – 52.13 μg/m^3. However, in Vietnam's National Technical Regulations, there is no regulation for the annual average threshold of O_3 (QCVN 05:2013/BTNMT), based on simulation results, all seven zones above have a relatively high annual average ground-level O_3 concentration, of which the highest is in zones six(CZ) and seven (CPZ) with average concentrations of 46.11 μg/m^3 and 46.41 μg/m^3, respectively, zone three (LXZ) had an average concentration of 44.70 μg/m^3 (1.04 times lower than that of CPZ); followed by zones four (HMZ) and five (TBZ) with average concentrations of 43.35 μg/m^3 and 43.19 μg/m^3 respectively (1.07 and 1.08 times lower than that if CPZ, respectively); and zones one (FAZ) and two (PRZ) had the lowest average concentrations across the entire MDR with 42.70 μg/m^3 and 41.83 μg/m^3 respectively (1.09 and 1.11 times lower than that of CPZ, respectively). In each zone, the average ground-level O_3 concentration tends to increase gradually from the inner delta to the coastal areas of the east and west coasts (especially the east coast and the southernmost at the tip of the South China Sea of Ca Mau province), from north to south, typically localities with concentrations > 48.5 μg/m^3 concentrated mainly in part of Tien Giang, Ben Tre, Tra Vinh, Soc Trang, and Bac Lieu provinces (about the east, southeast, and south) of zone six (CZ); the eastern and south-eastern parts of Ca Mau and Bac Lieu provinces in zone seven (CPZ); and the western and southwestern parts of Kien Giang province in zone one FAZ (west coastal area). The map of ground-level O_3 concentration by year and month is shown in Figures 3 and 4, respectively.

Figure 4. Spatio–temporal distribution of average ground-level O_3 concentration in 2018 in the Mekong Delta Region

Figure 5. Spatio–temporal distribution of average monthly ground-level O_3 concentrations in the MDR

3.2 Impacts of meteorological factors

The results of building a linear regression model between O_3 concentration (C_{O3}, y_i) and meteorological factors, including temperature x_1 (T, ^oK), relative humidity x_2 (RH, %), pressure surface pressure (or pressure for short) x_3 (P, Pa), and C_{O3} = F (T, RH, and P), are shown in Table 4. Regression calculation results shows that the correlation between temperature x_1, relative humidity x_2, and pressure x_3 for the value of O_3 concentration in six areas of the Mekong Delta has the form of (20) – (25), as follows:

Table 4. Calibrated equations C_{O3} = F (T, RH and P)

Agro-ecological zones	Regression equations	
Zone one, FAZ	$y_1 = -8,390.8243 + 3.0410x_1 + 0.6476x_2 + 7.4043x_3$ (20)	$R = 0.41700$
Zone two, PRZ	$y_2 = -8,236.7324 + 3.2776x_1 + 0.4885x_2 + 7.1928x_3$ (21)	$R = 0.42529$
Zone three, LXZ	$y_3 = -7,019.7334 + 3.2485x_1 + 0.6606x_2 + 5.9871x_3$ (22)	$R = 0.31874$
Zone five, TBZ	$y_4 = -7,547.9570 + 2.7163x_1 + 0.8825x_2 + 6.6471x_3$ (23)	$R = 0.36530$
Zone six, CZ	$y_5 = -10,019.9938 + 4.2081x_1 + 0.6320x_2 + 8.6748x_3$ (24)	$R = 0.43631$
Zone seven, CPZ	$y_6 = -8,898.4524 + 3.6720x_1 + 0.7786x_2 + 7.7107x_3$ (25)	$R = 0.36806$

Table 4. Correlation equation C_{O3} = F(T, RH and P)

The correlation coefficients for the three meteorological factors in the six zones are R_{FAZ}=0.417000, R_{PRZ}=0.42529, R_{LXZ}=0.31874, R_{TBZ}=0.36530, R_{CZ}=0.43631, and R_{CPZ}=0.36806. In all six zones of the MDR, the O_3 concentration values tended to increase to 3.0410 μg/m^3, 3.2776 μg/m^3, 3.2485 μg/m^3, 2.7163 μg/m^3, 4.2081 μg/m^3 and 4,849 μg/m^3 for every 1 unit (1 ^{o}K) increase in temperature (T), respectively (when relative humidity (RH) and surface pressure (P) remained unchanged). Similarly, for every 1 unit (1%) increase in RH, the O_3 concentration tends to increase by 0.6476 μg/m^3, 0.4885 μg/m^3, 0.6606 μg/m^3, 0.8825 μg/m^3, 0.6320 μg/m^3, and 0.7786 μg/m3, respectively (when T and P do not change), while P also has a similar positive effect when for every 1 unit (1 Pa) of P changes in an increasing direction, the O_3 concentration also tended to increase to 7.4043 μg/m^3, 7.1928 μg/m^3, 5.9871 μg/m3, 6.6471 μg/m^3, 8.6748 μg/m^3, and 7.7107 μg/m^3, respectively (when RH and T remained unchanged). Thus, all three meteorological factors, temperature, relative humidity, and surface pressure contribute to the increase in O_3 concentration, in which surface pressure and temperature reflect the most significant impact of varying complexity depending on the geographical region.

Based on the results of the univariate analysis of each meteorological factor (Table S27), the correlation coefficient (R) of P was the highest in areas two (PRZ) and six (CZ) with an explanatory level of approximately 16.60% and 16.82%, respectively, and the R of T was highest in areas one (FAZ), six (CZ), and seven (CPZ).

The results of multivariable regression calculated at p-*value* show when considering all three meteorological factors mentioned above, are T, RH, and P for O_3 concentration in the above six zones of the Mekong Delta; only the relative humidity RH and surface pressure P were statistically significant for (1) zone one (FAZ), zone three (LXZ), and zone five (TBZ; and (2) all three factors above were statistically

significant in zone two (PRZ), zone six (CZ), and zone seven (CPZ),. Thus, in zones one (FAZ), three (LXZ), and five (TBZ), there were at least two meteorological factors (relative humidity and surface pressure) that were independent with significant predictive significance value of O_3 concentration in these three zones. In zones two (PRZ), six (CZ), and seven (CPZ), all three meteorological factors above had a significant influence on the O_3 concentration in each zone (Table 5).

Table 5. Values in univariate linear regression analysis in 06 zone in the MDR of $C_{O3} = F(T)$, $C_{O3} = F(RH)$ và $C_{O3} = F(P)$

Factors	*α*	*β*	*R*	R^2	*p-value*
Agro-ecological zone one, FAZ					
Temperature, T	1,105.1139	-3.5342	0.14782	0.02185	0.00465
Relative humidity , RH	42.6918	-0.0020	0.00058	0.000001	0.99118
Surface pressure, P	-5,907.9236	5.8983	0.39190	0.15359	0.00000
Agro-ecological zone two, PRZ					
Temperature, T	361.0229	-1.0616	0.04037	0.00163	0.44195
Relative humidity , RH	72.0278	-0.4099	0.12546	0.01574	0.01648
Surface pressure, P	-5,844.6621	5.8349	0.40747	0.16603	0.00000
Agro-ecological zone three, LXZ					
Temperature, T	820.1010	-2.5780	0.10060	0.01012	0.05484
Relative humidity , RH	34.5034	0.1346	0.03568	0.00127	0.49683
Surface pressure, P	-4,519.9515	4.5264	0.28588	0.08173	0.00000
Agro-ecological zone five, TBZ					
Temperature, T	1,066.2555	-3.4042	0.13314	0.01773	0.01089
Relative humidity , RH	25.2459	0.2347	0.06487	0.00421	0.21634
Surface pressure, P	-4,785.1857	4.7847	0.30798	0.09485	0.00000
Agro-ecological zone six, CZ					
Temperature, T	922.5689	-2.9204	0.11804	0.01393	0.02411
Relative humidity , RH	70.4457	-0.3128	0.06129	0.00376	0.24276
Surface pressure, P	-6,706.8905	6.6923	0.41012	0.16820	0.00000
Agro-ecological zone seven, CPZ					
Temperature, T	948.9186	-3.0068	0.12607	0.01589	0.01596
Relative humidity , RH	29.0441	0.2193	0.06176	0.00381	0.23922
Surface pressure, P	-5,820.2431	5.8132	0.32643	0.10655	0.00000

Table 5. Values in univariate linear regression analysis in 06 zone in the MDR of C_{O3} = F(T), C_{O3} = F(RH) và C_{O3} = F(P)

3.3 Impacts of precursor emission factors

The indicators for O_3 concentration were C_{O3}, and $y_{2,j}$; CH_4 precursor emissions were E_{CH4}, x_1; CO was E_{CO}, x_2; NO_x was E_{NOx}, x_3; NMVOCs were E_{NMVOCs}, x_4; other VOCs were EO $_{ther\text{-}VOCs}$, x_5. The results of the multivariable regression equations C_{O3}=F (E_{CH4}, E_{CO}, E_{NOx}, E_{NMVOCs}, and $E_{Other\text{-}VOCs}$) (Table 6), show the multivariable correlation of precursor emissions (x_1, x_2, x_3, x_4, and x_5) and the value of O_3 concentration in the six zones of the Mekong Delta ($y_{2,j}$) has the form of (26)– (31), as follows:

Table 6. Multivariable correlation equation C_{O3} = F (E_{CH4}, E_{CO}, E_{NOx}, E_{NMVOCs} , $E_{Other\text{-}VOCs}$)

Agro-ecological zones	Regression equations	
Zone one, FAZ	$y_{2,1} = -48.2486 + 0.0030x_1 - 0.0010x_2 - 0.0214x_3 - 0.0008x_4 + 0.1689x_5$ (26)	$R_1 = 0.27185$
Zone two, PRZ	$y_{2,2} = 103.2945 + 0.7155x_1 - 0.7555x_2 + 15.7726x_3 + 0.1063x_4 + 9.1465x_5$ (27)	$R_2 = 0.54097$
Zone three, LXZ	$y_{2,3} = 174.5402 + 0.2784x_1 - 0.2472x_2 + 4.2370x_3 + 0.0181x_4 + 4.0573x_5$ (28)	$R_3 = 0.35830$
Zone five, TBZ	$y_{2,4} = 130.9500 + 0.0580x_1 - 0.0504x_2 + 0.8504x_3 + 0.0086x_4 + 0.4920x_5$ (29)	$R_4 = 0.27282$
Zone six, CZ	$y_{2,5} = 79.6082 + 0.0707x_1 - 0.0520x_2 + 0.5965x_3 + 0.0235x_4 + 0.5515x_5$ (30)	$R_5 = 0.38376$
Zone seven, CPZ	$y_{2,6} = -35.1283 + 0.0290x_1 - 0.0143x_2 - 0.0246x_3 + 0.0028x_4 + 1.4978x_5$ (31)	$R_6 = 0.25777$

Table 6. Multivariable correlation equation C_{O3} = F (E_{CH4}, E_{CO}, E_{NOx}, E_{NMVOCs} , $E_{Other\text{-}VOCs}$)

From the equations in Table 6, common correlation coefficient in the six partitioned zones have the values of R_1=0.27185, R_2=0.54097, R_3=0.35830, R_4=0.27282, R_5= 0.38376, and R_6=0.25777, respectively. O_3 concentration values in zones two (PRZ), three (LXZ), five (TBZ) and six(CZ) tended to increase for

every 1 unit (1 kg/day); the emissions of CH_4 or NO_x or NMVOCs or Other VOCs increased (when the remaining 04 precursors remained unchanged). Specifically, the O_3 concentration for E_{CH4} increased by 0.7155 µg/m^3, 0.2874 µg/m^3, 0.0580 µg/m^3, and 0.0707 µg/m^3 respectively; the O_3 concentration for E_{NOx} increased by 15.7726 µg/m^3, 4.2370 µg/m^3, 0.8504 µg/m^3, and 0.5965 µg/m^3 respectively. The O_3 concentrations for E_{NMVOCs} increased by 0.1063 µg/m^3, 0.0181 µg/m^3, 0.0086 µg/m^3, and 0.0235 µg/m^3 respectively; the O_3 concentrations for $E_{Other\text{-}VOCs}$, increased by 9,1465 µg/m^3, 4.0573 µg/m^3, 0.4920 µg/m^3, and 0.5515 µg/m^3, respectively. In contrast, the O_3 concentration in these four zones tended to decrease for every 1 unit (1 kg/day) of CO emissions increased (when the remaining four precursors remained unchanged); specifically, the O_3 concentration for E_{CO} decreased by 0.7555 µg/m^3, 0.2472 µg/m^3, 0.0504 µg/m^3, and 0.0520 µg/m^3, respectively. Meanwhile, the O_3 concentration in zone one (FAZ) tended to increase for every 1 unit (1 kg/day) of CH_4 or Other VOCs emissions increase (when the remaining four precursors were unchanged), were 0.0030 µg/m^3 and 0.1689 µg/m^3, respectively, which = was opposite to the change in emissions of CO, NO_x, or NMVOCs (when the remaining four precursors are unchanged), the O_3 concentration decreased by 0.0010 µg/m^3, 0.0214 µg/m^3, and 0.0008 µg/m^3, respectively. The O_3 concentration in zone seven (CPZ) tended to increase for every 1 unit (1 kg/day) of CH_4 or NMVOCs, or Other VOCs emissions increases (when the remaining four precursors were unchanged), were 0.0290 µg/m^3, 0.0028 µg/m^3, and 1.4978 µg/m^3, respectively. This was opposite to the change in emissions of CO or NO_x (when the remaining four precursors were unchanged), the O_3 concentration decreased by 0.0143 µg/m^3 and 0.0246 µg/m^3, respectively.

Thus, the precursors CH_4, NO_x, NMVOCs, and Other VOCs all contributed to the increase in O_3 concentrations in the PRZ, LXZ, TBZ, and CZ zones. Meanwhile, CH_4 and Other VOCs reflect the impact of increasing O_3 concentrations in only two areas, FAZ and CPZ. However, CO is the main factor reflecting the level of impact on reducing O_3 concentrations in the Mekong Delta, depending on certain geographical areas.

Based on the results of univariate analysis of each type of precursor emission, the correlation coefficient (R) of E_{CH4}, E_{CO}, and E_{NOx} was highest in zone two (PRZ) with explanatory levels of approximately 1.06%, 1.13%, and 1.20%, respectively, while the R of E_{NMVOCs} and $E_{Other\text{-}VOCs}$ was highest in zone seven (CPZ) with explanatory levels of approximately 1.10% and 0.28%, respectively. The results of multivariate regression calculated at p-*value* showed that: (1) zone one (FAZ) where E_{CH4} and $E_{Other\text{-}VOCs}$ were statistically significant (p-*value* < 0.05); (2) zone two (PRZ), all E_{CH4}, E_{CO}, E_{NOx}, E_{NMVOCs}, and $E_{Other\text{-}VOCs}$ were statistically significant; (3) zone 3 (LXZ), where E_{CH4}, E_{CO}, and E_{NOx} were statistically significant; (4) zone five (TBZ), where E_{CH4}, E_{CO}, E_{NOx}, and E_{NMVOCs} were statistically significant; (5) zone six CZ where E_{CH4}, E_{CO}, and E_{NMVOCs} were statistically significant; and (6) zone seven (CPZ), where only $E_{Other\text{-}VOCs}$ were statistically significant. Thus, in the six zones in the MDR, emissions of precursors E_{CH4}, E_{CO}, E_{NOx}, and E_{NMVOCs} were independent factors that affect the O_3 concentration in these six zones. Meanwhile, Other-

VOCs precursor emissions had little or no influence on the O_3 concentrations in each zone of the MDR (Table 7)

Table 7. Synthesis of values in univariate linear regression analysis in 06 areas in the Mekong Delta of $C_{O3} = F(E_{CH4})$, $C_{O3} = F(E_{CO})$, $C_{O3} = F(E_{NOx})$, $C_{O3} = F(E_{NMVOCs})$ và $C_{O3} = F(E_{Other\text{-}VOCs})$

Factors	α	β	R	R^2	p-value
Agro-ecological zone one, FAZ					
E_{CH4}	44.05661	-0.00002	0.03943	0.00155	0.45267
E_{CO}	45.13400	-0.00001	0.04738	0.00224	0.36677
E_{NOx}	48.28175	-0.00072	0.06223	0.00387	0.23562
E_{NMVOCs}	46.85881	-0.00011	0.03381	0.00114	0.51962
$E_{Other\text{-}VOCs}$	28.80561	0.00859	0.01455	0.00021	0.78177
Agro-ecological zone two, PRZ					
E_{CH4}	44.63183	-0.00016	0.10313	0.01064	0.04897
E_{CO}	45.21684	-0.00008	0.10614	0.01127	0.04270
E_{NOx}	45.59218	-0.00354	0.10963	0.01202	0.03629
E_{NMVOCs}	45.70085	-0.00045	0.06037	0.00364	0.24994
$E_{Other\text{-}VOCs}$	27.64205	0.29087	0.01741	0.00030	0.74023
Agro-ecological zone three, LXZ					
E_{CH4}	42.91945	0.00027	0.04816	0.00232	0.35886
E_{CO}	42.77637	0.00012	0.04382	0.00192	0.40387
E_{NOx}	42.71862	0.00500	0.04275	0.00183	0.41552
E_{NMVOCs}	46.66667	-0.00070	0.02875	0.00083	0.58405
$E_{Other\text{-}VOCs}$	68.13774	-0.99878	0.02694	0.00073	0.60789
Agro-ecological zone five, TBZ					
E_{CH4}	41.36059	0.00010	0.04663	0.00217	0.37439
E_{CO}	41.10480	0.00004	0.04162	0.00173	0.42793
E_{NOx}	41.07626	0.00162	0.03834	0.00147	0.46529
E_{NMVOCs}	39.56914	0.00044	0.03403	0.00116	0.51697
$E_{Other\text{-}VOCs}$	-4.65496	0.35598	0.03781	0.00143	0.47149
Agro-ecological zone six, CZ					

Factors	α	β	R	R^2	p-value
E_{CH4}	47.21390	-0.00007	0.03172	0.00101	0.54578
E_{CO}	47.71331	-0.00004	0.03653	0.00133	0.48655
E_{NOx}	48.28819	-0.00199	0.04293	0.00184	0.41352
E_{NMVOCs}	43.43907	0.00039	0.02206	0.00049	0.67440
$E_{Other\text{-}VOCs}$	-3.41572	0.44490	0.03716	0.00138	0.47909
Agro-ecological zone seven, CPZ					
E_{CH4}	44.13394	0.00016	0.05080	0.00258	0.33314
E_{CO}	43.74877	0.00007	0.04686	0.00220	0.37203
E_{NOx}	44.40019	0.00128	0.02032	0.00041	0.69882
E_{NMVOCs}	30.86259	0.00198	0.10508	0.01104	0.04483
$E_{Other\text{-}VOCs}$	-22.89717	0.55705	0.05261	0.00277	0.31619

Table 7. Synthesis of values in univariate linear regression analysis in 06 zones in the MDR of $C_{O3}=F(E_{CH4})$, $C_{O3}=F(E_{CO})$, $C_{O3}=F(E_{NOx})$, $C_{O3}=F(E_{NMVOCs})$ and $C_{O3}=F(E_{Other\text{-}VOCs})$

3.4 Synthetic impacts of precursor emission and meteorological factors

A multivariable experimental linear regression model was built to evaluate the overall relationship between O_3 concentration (C_{O3}, $y_{3,j}$) and meteorological factors, including temperature value x_1 (T, ^oK), relative humidity x_2 (RH, %), surface pressure x_3 (P, Pa), and the types of CH_4 precursor emissions were E_{CH4}, x_4; CO was E_{CO}, x_5; NO_x was E_{NOx}, x_6; NMVOCs were E_{NMVOCs}, x_7; and Other VOCs were $_{EOther\text{-}VOCs}$, x_8. This result is shown in Table 8, along with (32) – (37).

Table 8. Multivariable correlation equation C_{O3} = F (T, RH, P, E_{CH4}, $E_{CO,}$ E_{NOx}, E_{NMVOCs} , $E_{Other\text{-}VOCs}$)

Table 8. Multivariable correlation equation C_{O3} = F (T, RH, P, E_{CH4}, $E_{CO,}$ E_{NOx}, E_{NMVOCs} , $E_{Other\text{-}VOCs}$)

Agro-ecological zones	Regression equations
	$+9.0456x_6 + 0.0396x_7 + 4.1520x_8$ **(34)**, $\boldsymbol{R_3 = 0.53909}$
Zone five, TBZ	$y_{3,4} = -7,884.0483 - 0.9500x_1 + 0.4803x_2 + 8.1701x_3 + 0.0369x_4 - 0.0381x_5$ $+0.8014x_6 + 0.0037x_7 - 0.0224x_8$ **(35)**, $\boldsymbol{R_4 = 0.46066}$
Zone six, CZ	$y_{3,5} = -7,417.1310 + 0.7628x_1 + 0.4705x_2 + 7.1752x_3 + 0.0679x_4 - 0.0603x_5$ $+1.0122x_6 + 0.0178x_7 + 0.0002x_8$ **(36)**, $\boldsymbol{R_5 = 0.47874}$
Zone seven, CPZ	$y_{3,6} = -9,307.2703 + 2.4693x_1 + 0.7901x_2 + 8.4274x_3 + 0.0079x_4 - 0.0033x_5$ $-0.0107x_6 - 0.0012x_7 + 0.6200x_8$ **(37)**, $\boldsymbol{R_5 = 0.42218}$

Table 8 shows that the common correlation coefficients at six partitioned zones were R_1=0.47549, R_2=0.61360, R_3=0.53909, R_4=0.46066, R_5=0.47874 and R_6=0.42218, respectively. For zone one (FAZ), the factors of RH, P, and the emissions of E_{NOx}, E_{NMVOCs} and $_{EOther\text{-}VOCs}$ affect the distribution of O_3 concentration in the zone; for zone two (PRZ), these are P, emissions of E_{CH4}, E_{CO}, E_{NOx}, E_{NMVOCs} and $_{EOther\text{-}VOCs}$. For zone three (LXZ), P, E_{CH4}, E_{CO}, E_{NOx}, and E_{NMVOCs} emissions; (4) for zone five (TBZ), P, emissions E_{CH4}, E_{CO}, and E_{NOx}; for zone six (CZ), P, emissions E_{CH4}, E_{CO}, E_{NOx}, and E_{NMVOCs}. Finally, in zone 7 (CPZ), the RH and P were the main independent factors with a major predictive significance for the individual O_3 concentration value for the six zones partitioned in MDR.

3.5 Uncertainty analysis

These limitations could lead to uncertainty in the research results and create errors in the simulation evaluation of ground-level O_3 concentration distribution. This could be explained in detail, first, by the limitation in the ground-level O_3 concentration monitoring data and the field data measured at

meteorological observation stations in the MDR. For ground-level O_3 concentration measurement data in the entire MDR, there was no monitoring station to measure the ground-level O_3 concentration (it only monitored some basic pollution indicators, such as TSP, SO_2, NO_x, CO, and PM_{10}). The dataset in this study was collected from monitoring stations in the vicinity of Binh Duong Province, which was also an area within simulation domain D02 covering the entire study area. The ground-level O_3 concentration measurement dataset was created by the observation method, which was performed manually, and measured only four times at 9:00, 11:00, 13:00, and 15:00 on an important day unique monitoring at each station from January, 2018, to December, 2018.

Second, the contribution of the emission of two main precursors of NO_x and NMVOCs in each group of industries/activities was different among zones in the Mekong Delta, especially in zones one (FAZ), two (PRZ), five (TBZ), six (CZ), and seven (CPZ), with a of 520–1,530 thousand hectares compared to zone three (LXZ), and zone four (HMZ) with an area of only 95–225 thousand hectares. Significant differences in socio-economic activities, management levels of each locality, and the difference in soil problems by geographical zone (between freshwater alluvial soils and acid and saline soils) led to an assessment of six zones (not considering the four HMZ zones), which may not fully reflect the level of detail according to the administrative management level in each zone. Moreover, the 2018 emission inventory dataset built for the entire region (range of calculation D02) had a low resolution and a relatively large grid size (approximately 9.5 km) and natural emissions from forest fires in zones five (TBZ) and seven (CPZ) were not considered due to lack of detailed inventory data during the simulation.

Third, the correlations were limited to evaluation in the form of a multivariable linear function between O_3 concentration and meteorological factors; the main precursor emissions were NO_x and NMVOCs. In this study, correlation of some forms of VOC precursor components according to the chemical mechanism of the CMAQ model was not performed. Moreover, the three selected meteorological factors, including temperature, relative air humidity, and surface pressure, cannot fully account for the impact of meteorology on the formation of O_3. As a result, the correlation level is not high enough (R only reaches a maximum of 0.61 in the two LXZ areas).

Fourth, in the MLR multivariable linear function models between total ground-level O_3 concentration and meteorological factors combined with emission precursors, the interaction between variables (combination of quadratic or ternary variables) increased the confidence level of the analytical model.

4 Discussion

The seasonal variation of ground-level O_3 was noted in many regions of the world (Maji et al., 2019) (Tang et al., 2013), (Simon et al., 2012) in MDR, the change in ground-level O_3 concentration is quite complicated according to the season; in the dry season, the O_3 concentration is generally higher than that in the wet season with O_3 values. In the month with highest concentration of the dry season, February, the 1-hour average concentration ranged from 17.2 μg/m^3 to 102.1 μg/m^3, which was still significantly lower

than the allowable limit of QCVN 05:2013/BTNMT (hourly average with 200 μg/m^3), but different effects on crops should be considered. During the wet season, the highest O_3 value in the transitional period at the end of the season (October) ranged from 8.6 μg/m^3 to 117.4 μg/m^3. Considering the monthly average, the O_3 concentration was high (> 60 μg/m^3), occurring in February, June, October, and December. In January, March–May, and July–September, the concentration level was much lower than in August (wet season), with the lowest concentration in the range of 16.7–25.1 μg/m^3. October (end of the wet season) had the highest monthly average concentration, ranging from 55.4 μg/m^3 to 84.5 μg/m^3. The spatial distribution trend of terrestrial O_3 concentration shows that there is a clear and gradual shift from the inner delta to the eastern coastal areas in zone six (CZ), Cape Ca Mau in zone seven (CPZ), and the western coastal areas of zone 1 (FAZ) in Kien Giang Province.

Figure 6. Emission distribution of two precursors NO_x and NMVOCs with major impacts on ozone pollution in the Mekong Delta Region.

The role of precursors in the distribution of ozone concentrations has been discussed in similar studies (Xue et al., 2014; Sharma et al., 2016; Han et al., 2019; Chen et al., 2021;Mousavinezhad et al., 2021; Mitchell et al., 2021). The modelling results showed that the two precursors of NO_x and NMVOCs were the main contributors to ground-level O_3 pollution. These two precursors originate from anthropogenic activities as well as natural biological sources, with the largest contribution coming from zone one (FAZ) with 91.5 thousand tons of NO_x/year and 455.2 thousand tons of NMVOCs/year, followed by zone two (PRZ), zone seven (CPZ), zone five (TBZ), zone six CZ, and zone three (LXZ); the lowest was in zone four (HMZ) (Fig. 6). In particular, the NMVOCs precursors in each zone had a significant impact and were much more sensitive than the NO_x precursor emissions with the NMVOCs/NO_x ratio in zone one (FAZ) of 4.97, zone two (PRZ) was 8.03 times, zone three (LXZ) was 7.84 times; zone four (HMZ) was 6.82 times, zone five (TBZ) was 6.55 times, zone six (CZ) was 5.50 times and zone seven (CPZ) was 5.55 times. The pollution contribution was predominantly from anthropogenic activities with three main groups of industries/activities in the following order: (1) industrial production activities, (2) activities from residential zones and people's livelihood, and (3) agricultural production activities such as rice and crop cultivation, using land, livestock, etc.

Meteorology is one of the factors that directly affect the distribution of ground – level ozone concentration (Camalier et al., 2007; Davis et al., 2011; Godowitch et al., 2015; Mousavinezhad et al., 2021). The results showed that relative humidity (RH) and surface pressure (P) were the two main factors contributing to the increase in ground-level O_3 concentration, specifically, the increase in ground-level O_3 concentration from 5.9–8.7 μg/m^3/Pa with each pressure unit increase (when temperature and relative humidity did not change) respectively for zone three (LXZ), zone five (TBZ), zone two (PRZ), zone one (FAZ), zone seven (CPZ) and zone six (CZ); and from 0.5–0.9 μg/m^3/ % with each unit of humidity increase (when surface temperature and pressure remain unchanged) for zones two (PRZ), zone six (CZ), zone one (FAZ), zone three (LXZ), zone seven (CPZ) and zone five (TBZ), respectively. Moreover, the

correlations between the ground-level O_3 concentration values and NO_x and NMVOCs precursor emissions were statistically significant ($p < 0.05$), showing that they contributed to the increase in ground-level O_3 concentration in zones two (PRZ), three (LXZ), five (TBZ), and six (CZ), whereas this is the opposite in zones one (FAZ) and seven (CPZ). At the same time, when evaluating the correlations between the ground-level O_3 concentration and meteorological factors combined with precursor emissions, the correlation index (R) gives results that are at a satisfactory level with values fluctuating from 0.42 to 0.61 ($R > 0.4$).

5 Conclusion

The MDR has a strategic location in Vietnam, bordering the East Sea and the Southwest Sea, the exclusive economic zone on the east, west, and south. It has a very favourable environment for growing rice, an important food crop globally. Rapid industrialisation in the Mekong Delta has increased the trend of ground – level zone concentrations, leading to a decline in crop yields. The distribution of ozone concentration for a year was modelled to determine the dependence of ozone concentration on emission factors and meteorology. Using a combination of WRF/CMAQ and multiple linear regression models, the following results were obtained.

First, the ground-level O_3 concentration during the dry season was higher than that in the wet season; the month with the highest concentration reaches an average concentration of 1 h, ranging from 17.2 $\mu g/m^3$ to 102.1 $\mu g/m^3$. In the wet season, the O_3 value was highest at the end of October, reaching 8.6–117.4 $\mu g/m^3$. Within the Mekong Delta, ground-level ozone concentrations ranged from 40.39 $\mu g/m^3$ to 52.13 $\mu g/m^3$.

Second, the Mekong Delta was divided into six agro-ecological zones corresponding to geographical features, agriculture, and water resources: the FAZ, PRZ, LXZ, TBZ, CZ, and CPZ. The two precursors of NO_x emissions and NMVOCs are major contributors to terrestrial O_3 pollution. The largest contribution of emissions comes from FAZ with 91.5 thousand tons of NO_x/year and 455.2 thousand tons of NMVOCs/year. Next, is zone two (PRZ), zone seven (CPZ), zone five (TBZ), zone six (CZ), and the lowest was zone four (mountainous).

Third, in each zone, the NMVOCs precursors have a significant impact and are much more sensitive than the NO_x precursor emissions with the NMVOCs/NOx ratio in the first zone (FAZ) of 4.97, respectively. times, zone 2 (PRZ) is 8.03 times, zone 3 (LXZ) is 7.84 times; zone 4 (HMZ) is 6.82 times, zone 5 (TBZ) is 6.55 times, zone 6 (CZ) is 5.50 times and zone 7 (CPZ) is 5.55 times. Anthropogenic activities were the main sources of pollution, from three main groups of industries/activities in the following order: (1) industrial production activities, (2) residential zones and people's livelihood activities, and (3) from agricultural production activities such as rice and crop cultivation, using land, livestock, etc.

Fourth, in the sixth zone, the emissions of precursors E_{CH4}, E_{CO}, E_{NOx}, and E_{NMVOCs} were independent factors mainly affecting the ground-level O_3 concentration in these six zones. Other-VOCs precursor emissions had little or no influence on the O_3 concentration values in each area of the MDR.

Fifth, humidity (RH) and surface pressure (P) were the two main meteorological factors that contributed to the increase in O_3 concentration, among the three meteorological factors considered in this study, the humidity (RH), surface pressure (P), and temperature (T).

Declarations

Ethical Approval

The authors declare :

The manuscript is not submitted to more than one journal for simultaneous consideration.

The manuscript is original and not have been published elsewhere in any form or language (partially or in full), unless the new work concerns an expansion of previous work.

The manuscript is not split up into several parts to increase the quantity of submissions and submitted to various journals or to one journal over time (i.e. 'salami-slicing/publishing').

Results are presented clearly, honestly, and without fabrication, falsification or inappropriate data manipulation. We adhere to discipline-specific rules for acquiring, selecting and processing data.

We have provided all data and proper mentions of other works

Consent to Participate

I consent to participate publish my manuscript entitled "*Ground-level ozone in Mekong delta region: precursors, meteorological factors, and regional transport*" to the Environmental Science and Pollution Research (ESPR).

Consent to Publish

I consent to publish my manuscript entitled "*Ground-level ozone in Mekong delta region: precursors, meteorological factors, and regional transport*" to the Environmental Science and Pollution Research (ESPR).

Authors Contributions

Long Ta Bui: Conceptualization, Funding acquisition, Investigation, Project administration, Resources, Supervision, Methodology, Models, writing - original draft, writing - review \& editing.

Phong Hoang Nguyen: Data curation, Data analysis, Formal analysis, Validation,GIS

Funding

We acknowledge the support of time and facilities from Ho Chi Minh City University of Technology (HCMUT), VNU- HCM for this study.

Competing Interests

The authors declare that they have no known competing financial interests or personal relationships that could have appeared to influence the work reported in this paper.

Availability of data and materials

We declare that all data relating to this manuscript are truthful and we will gladly share it with any interested readers or at the request of the editor board.

References

1. Arshad A (2021) A growth and biochemistry of ten high yielding genotypes of Pakistani rice (Oryza sativa L.) at maturity under elevated tropospheric ozone. Heliyon 7(10):e08198. https://doi.org/10.1016/j.heliyon.2021.e08198
2. Astitha M, Luo H, Rao ST, Hogrefe C, Mathur R, Kumar N (2017) Dynamic evaluation of two decades of WRF-CMAQ ozone simulations over the contiguous United States. Atmos Environ 164:102–116. https://doi.org/10.1016/j.atmosenv.2017.05.020
3. Avnery S, Mauzerall DL, Liu J, Horowitz LW (2011) Global crop yield reductions due to surface ozone exposure: 1. Year 2000 crop production losses and economic damage. Atmos Environ 45(13):2284–2296. https://doi.org/10.1016/j.atmosenv.2010.11.045
4. Bich Tho LC, Umetsu C (2022) Sustainable farming techniques and farm size for rice smallholders in the Vietnamese Mekong Delta: A slack-based technical efficiency approach. *Agriculture, Ecosystems and Environment*, *326*(August 2021), 107775. https://doi.org/10.1016/j.agee.2021.107775
5. Binh Duong CEM (2019) Report on the current state of air environment in Binh Duong province in 2018. CEM. (in Vietnamse)
6. Biswas DK, Xu H, Li YG, Liu MZ, Chen YH, Sun JZ, Jiang GM (2008) Assessing the genetic relatedness of higher ozone sensitivity of modern wheat to its wild and cultivated progenitors/relatives. J Exp Bot 59(4):951–963. https://doi.org/10.1093/jxb/ern022
7. Borge R, Lumbreras J, Pérez J, de la Paz D, Vedrenne M, de Andrés JM, Rodríguez ME (2014) Emission inventories and modeling requirements for the development of air quality plans. Application to Madrid (Spain). Sci Total Environ 466–467:809–819. https://doi.org/10.1016/j.scitotenv.2013.07.093
8. Brunekreef B, Holgate ST (2002) Air pollution and health. Lancet 360(9341):1233–1242. https://doi.org/10.1016/S0140-6736(02)11274-8

9. Camalier L, Cox W, Dolwick P (2007) The effects of meteorology on ozone in urban areas and their use in assessing ozone trends. Atmos Environ 41(33):7127–7137. https://doi.org/10.1016/j.atmosenv.2007.04.061
10. Carter CA, Cui X, Ding A, Ghanem D, Jiang F, Yi F, Zhong F (2017) Stage-specific, Nonlinear Surface Ozone Damage to Rice Production in China. Sci Rep 7(February):6–11. https://doi.org/10.1038/srep44224
11. Cha-um S, Vejchasarn P, Kirdmanee C (2007) An effective defensive response in Thai aromatic rice varieties (Oryza sativa L. spp. indica) to salinity. J Crop Sci Biotechnol 10(4):257–264. http://www.cropbio.org/contribute/paperfiles/Chalermpol Kirdmanee.pdf
12. Chen Y, Han H, Zhang M, Zhao Y, Huang Y, Zhou M, Wang C, He G, Huang R, Luo B, Hu Y (2021) Trends and variability of ozone pollution over the mountain-basin areas in Sichuan province during 2013–2020: Synoptic impacts and formation regimes. Atmosphere 12(12):1–15. https://doi.org/10.3390/atmos12121557
13. Chen Z, Wang X, Feng Z, Zheng F, Duan X, Yang W (2008) Effects of elevated ozone on growth and yield of field-grown rice in Yangtze River Delta, China. J Environ Sci 20(3):320–325. https://doi.org/10.1016/S1001-0742(08)60050-9
14. Cramb R (2020) White gold: The commercialisation of rice farming in the lower mekong basin. White Gold: The Commercialisation of Rice Farming in the Lower Mekong Basin 1–456. https://doi.org/10.1007/978-981-15-0998-8
15. Crippa M, Guizzardi D, Muntean M, Schaaf E, Dentener F, Van Aardenne JA, Monni S, Doering U, Olivier JGJ, Pagliari V, Janssens-Maenhout G (2018) Gridded emissions of air pollutants for the period 1970–2012 within EDGAR v4.3.2. Earth Syst Sci Data 10(4):1987–2013. https://doi.org/10.5194/essd-10-1987-2018
16. Danh NT, Huy LN, Oanh NTK (2016) Assessment of rice yield loss due to exposure to ozone pollution in Southern Vietnam. Sci Total Environ 566–567:1069–1079. https://doi.org/10.1016/j.scitotenv.2016.05.131
17. Davis J, Cox W, Reff A, Dolwick P (2011) A comparison of CMAQ-based and observation-based statistical models relating ozone to meteorological parameters. Atmos Environ 45(20):3481–3487. https://doi.org/10.1016/j.atmosenv.2010.12.060
18. Decock C, Six J (2012) Effects of elevated CO 2 and O 3 on N-cycling and N 2O emissions: A short-term laboratory assessment. Plant Soil 351(1–2):277–292. https://doi.org/10.1007/s11104-011-0961-1
19. Doliente SS, Samsatli S (2021) Integrated production of food, energy, fuels and chemicals from rice crops: Multi-objective optimisation for efficient and sustainable value chains. J Clean Prod 285:124900. https://doi.org/10.1016/j.jclepro.2020.124900
20. Eder B, Yu S (2006) A performance evaluation of the 2004 release of Models-3 CMAQ. Atmos Environ 40(26):4811–4824. doi: 10.1016/j.atmosenv.2005.08.045

21. Emberson LD, Büker P, Ashmore MR, Mills G, Jackson LS, Agrawal M, Atikuzzaman MD, Cinderby S, Engardt M, Jamir C, Kobayashi K, Oanh NTK, Quadir QF, Wahid A (2009) A comparison of North American and Asian exposure–response data for ozone effects on crop yields. Atmos Environ 43(12):1945–1953. https://doi.org/10.1016/j.atmosenv.2009.01.005
22. Emery Z, Liu AG, Russell MT, Odman G, Yarwood, Kumar N (2017) "Recommendations on statistics and benchmarks to assess photochemical model performance," J. Air Waste Manage. Assoc., vol. 67, no. 5, pp. 582–598, Apr. doi: 10.1080/10962247.2016.1265027
23. Ene A, Dunarea U, Galati J, Enea ADM, Ss TS (2015) *AIR POLLUTION AND VEGETATION ICP Air Pollution and Vegetation*. *SEPTEMBER*
24. Epa U (2006) Air Quality Criteria for Ozone and Related Photochemical Oxidants Volume II of III. *Environmental Protection*, *I*(February), pp.820
25. Feng Z, Kobayashi K (2009) Assessing the impacts of current and future concentrations of surface ozone on crop yield with meta-analysis. Atmos Environ 43(8):1510–1519. https://doi.org/10.1016/j.atmosenv.2008.11.033
26. Ferrer AJG, Thanh LH, Kiet NT, Chuong PH, Trang VT, Hopanda JC, Carmelita BM, Gummadi S, Bernardo EB (2022) The impact of an adjusted cropping calendar on the welfare of rice farming households in the Mekong River Delta, Vietnam. Econ Anal Policy 73:639–652. https://doi.org/10.1016/j.eap.2021.12.018
27. Friberg MD, Zhai X, Holmes HA, Chang HH, Strickland MJ, Sarnat SE, Tolbert PE, Russell AG, Mulholland JA (2016) Method for Fusing Observational Data and Chemical Transport Model Simulations to Estimate Spatiotemporally Resolved Ambient Air Pollution. Environ Sci Technol 50(7):3695–3705. https://doi.org/10.1021/acs.est.5b05134
28. Garner GG, Thompson AM (2013) Ensemble statistical post-processing of the national air quality forecast capability: Enhancing ozone forecasts in Baltimore, Maryland. Atmos Environ 81:517–522. https://doi.org/10.1016/j.atmosenv.2013.09.020
29. Godowitch JM, Gilliam RC, Roselle Roselle SJ (2015) Investigating the impact on modeled ozone concentrations using meteorological fields from WRF with an updated four-dimensional data assimilation approach. Atmospheric Pollution Research 6(2):305–311. https://doi.org/10.5094/APR.2015.034
30. Granier C, Darras S, Van Der Gon D, Jana H, Elguindi D, Bo N, Michael G, Marc G, Jalkanen G, Kuenen J (2019) *The Copernicus Atmosphere Monitoring Service global and regional emissions (April 2019 version). Data from ECCAD*. *April*. https://doi.org/10.24380/d0bn-kx16
31. GSO GSO (2020) Result of the Vietnam Household Living Standards Survey 2019. Statistical Publishing House, Hanoi
32. Guo H, Chen K, Wang P, Hu J, Ying Q, Gao A, Zhang H (2019) Simulation of summer ozone and its sensitivity to emission changes in China. Atmospheric Pollution Research 10(5):1543–1552. https://doi.org/10.1016/j.apr.2019.05.003

33. Han BS, Baik JJ, Kwak KH (2019) A preliminary study of turbulent coherent structures and ozone air quality in Seoul using the WRF-CMAQ model at a 50 m grid spacing. Atmos Environ 218(April):117012. https://doi.org/10.1016/j.atmosenv.2019.117012
34. Hoesly RM, Smith SJ, Feng L, Klimont Z, Janssens-Maenhout G, Pitkanen T, Seibert JJ, Vu L, Andres RJ, Bolt RM, Bond TC, Dawidowski L, Kholod N, Kurokawa J, Li M, Liu L, Lu Z, Moura MCP, O'Rourke PR, Zhang Q (2018) Historical (1750–2014) anthropogenic emissions of reactive gases and aerosols from the Community Emissions Data System (CEDS). Geosci Model Dev 11:369–408. https://doi.org/10.5194/gmd-2017-43
35. Hu J, Wu L, Zheng B, Zhang Q, He K, Chang Q, Li X, Yang F, Ying Q, Zhang H (2015) Source contributions and regional transport of primary particulate matter in China. Environ Pollut 207:31–42. https://doi.org/10.1016/j.envpol.2015.08.037
36. Ishii S, Bell JNB, Marshall FM (2007) Phytotoxic risk assessment of ambient air pollution on agricultural crops in Selangor State, Malaysia. Environ Pollut 150(2):267–279. https://doi.org/10.1016/j.envpol.2007.01.012
37. Ishii S, Marshall FM, Bell JNB (2004) Physiological and morphological responses of locally grown Malaysian rice cultivars (Oryza sativa L.) to different ozone concentrations. Water Air Soil Pollut 155(1–4):205–221. https://doi.org/10.1023/B:WATE.0000026528.86641.5b
38. Knoben JE, Freer, Woods RA (2019) Technical note: Inherent benchmark or not? Comparing Nash–Sutcliffe and Kling–Gupta efficiency scores. Hydrol Earth Syst Sci 23(10):4323–4331. doi: 10.5194/hess-23-4323-2019
39. Lang J, Zhou Y, Chen D, Xing X, Wei L, Wang X, Zhao N, Zhang Y, Guo X, Han L, Cheng S (2017) Investigating the contribution of shipping emissions to atmospheric PM2.5 using a combined source apportionment approach. Environ Pollut 229:557–566. https://doi.org/10.1016/j.envpol.2017.06.087
40. Li X, Rappenglück B (2014) A WRF-CMAQ study on spring time vertical ozone structure in Southeast Texas. Atmos Environ 97:363–385. https://doi.org/10.1016/j.atmosenv.2014.08.036
41. Maji KJ, Ye WF, Arora M, Nagendra SMS (2019) Ozone pollution in Chinese cities: Assessment of seasonal variation, health effects and economic burden. Environ Pollut 247(x):792–801. https://doi.org/10.1016/j.envpol.2019.01.049
42. McCuen Z, Knight, Cutter AG (2006) Evaluation of the Nash–Sutcliffe Efficiency Index. J Hydrol Eng 11(6):597–602. doi: 10.1061/(asce)1084-0699(2006)11:6(597)
43. McNider RT, Pour-Biazar A (2020) Meteorological modeling relevant to mesoscale and regional air quality applications: a review. In *Journal of the Air and Waste Management Association* (Vol. 70, Issue 1). Taylor & Francis. https://doi.org/10.1080/10962247.2019.1694602
44. Mitchell M, Wiacek A, Ashpole I (2021) Surface ozone in the North American pollution outflow region of Nova Scotia: Long-term analysis of surface concentrations, precursor emissions and long-range transport influence. Atmos Environ 261:118536. https://doi.org/10.1016/j.atmosenv.2021.118536
45. Morris RE, Mc Nally DE, Tesche TW, Tonnesen G, Boylan JW, Brewer P (2005) Preliminary Evaluation of the Community Multiscale Air Quality Model for 2002 over the Southeastern United States. J Air

Waste Manag Assoc 55(11):1694–1708. doi: 10.1080/10473289.2005.10464765

46. Mousavinezhad S, Choi Y, Pouyaei A, Ghahremanloo M, Nelson DL (2021) A comprehensive investigation of surface ozone pollution in China, 2015–2019: Separating the contributions from meteorology and precursor emissions. *Atmospheric Research*, *257*(December 2020), 105599. https://doi.org/10.1016/j.atmosres.2021.105599
47. NCEP (2000) *CISL RDA: NCEP FNL Operational Model Global Tropospheric Analyses, continuing from July 1999*. National Centers for Environmental Prediction/National Weather Service/NOAA/U.S. Department of Commerce, 2000t
48. Nguyen T, Nagashima, Van Doan Q, Basel A (2020) vol. 11, no. 7, 2020, doi: 10.3390/atmos11070733
49. Nguyen DC, Le TD, Nguyen VS, Miller F (2007) *Livelihoods and Resource Use Strategies of Farmers in the Mekong Delta. In: Challenges to Sustainable Development in the Mekong Delta. Regional and National Policy Issues and Research Needs*
50. Nguyen MT, Renaud FG, Sebesvari Z (2019) Drivers of change and adaptation pathways of agricultural systems facing increased salinity intrusion in coastal areas of the Mekong and Red River deltas in Vietnam. Environ Sci Policy 92(July):331–348. https://doi.org/10.1016/j.envsci.2018.10.016
51. Nouchi I, Ito O, Harazono Y, Kobayashi K (1991) Effects of chronic ozone exposure on growth, root respiration and nutrient uptake of rice plants. Environ Pollut 74(2):149–164. https://doi.org/10.1016/0269-7491(91)90111-9
52. Olszyk DM, Wise C (1997) Interactive effects of elevated CO2 and O3 on rice and flacca tomato. Environment 66:1–10
53. Pleijel H (2011) Reduced ozone by air filtration consistently improved grain yield in wheat. Environ Pollut 159(4):897–902. https://doi.org/10.1016/j.envpol.2010.12.020
54. Ramya A, Dhevagi P, Rakesh SS, Maheswari M, Karthikeyan S, Saraswathi R, Chandrasekhar CN, Venkataramani S (2021) Detection of ozone stress in rice cultivars using spectral reflectance. Environ Adv 6:100129. https://doi.org/10.1016/j.envadv.2021.100129
55. Sarwar G, Luecken D, Yarwood G, Whitten GZ, WCarter WPL (2008) Impact of an updated carbon bond mechanism on predictions from the CMAQ modeling system: Preliminary assessment. J Appl Meteorol Climatology 47(1):3–14. https://doi.org/10.1175/2007JAMC1393.1
56. Senthilkumar N, Gilfether M, Metcalf F, Russell AG, Mulholland JA, Chang HH (2019) Application of a fusion method for gas and particle air pollutants between observational data and chemical transport model simulations over the contiguous United States for 2005–2014. Int J Environ Res Public Health 16(18). https://doi.org/10.3390/ijerph16183314
57. Shang B, Fu R, Agathokleous E, Dai L, Zhang G, Wu R, Feng Z (2022) Ethylenediurea offers moderate protection against ozone-induced rice yield loss under high ozone pollution. Sci Total Environ 806:151341. https://doi.org/10.1016/j.scitotenv.2021.151341

58. Sharma S, Chatani S, Mahtta R, Goel A, Kumar A (2016) Sensitivity analysis of ground level ozone in India using WRF-CMAQ models. Atmos Environ 131:29–40. https://doi.org/10.1016/j.atmosenv.2016.01.036
59. Simon H, Baker KR, Phillips S (2012) Compilation and interpretation of photochemical model performance statistics published between 2006 and 2012. Atmos Environ 61:124–139. https://doi.org/10.1016/j.atmosenv.2012.07.012
60. Simon H, Reff A, Wells B, Xing J, Frank N (2015) Ozone trends across the United States over a period of decreasing NOx and VOC emissions. Environ Sci Technol 49(1):186–195. https://doi.org/10.1021/es504514z
61. Skamarock WC, Klemp JB, Dudhi J, Gill DO, Barker DM, Duda MG, Huang X-Y, Wang W, Powers JG (2008) A Description of the Advanced Research WRF Version 3. *Technical Report*, *June*, 113. https://doi.org/10.5065/D6DZ069T
62. Sokhi RS, San José R, Kitwiroon N, Fragkou E, Pérez JL, Middleton DR (2006) Prediction of ozone levels in London using the MM5-CMAQ modelling system. Environ Model Softw 21(4):566–576. https://doi.org/10.1016/j.envsoft.2004.07.016
63. Tai APK, Mickley LJ, Jacob DJ (2010) Correlations between fine particulate matter (PM2.5) and meteorological variables in the United States: Implications for the sensitivity of PM2.5 to climate change. Atmos Environ 44(32):3976–3984. https://doi.org/10.1016/j.atmosenv.2010.06.060
64. Tang H, Liu G, Zhu J, Han Y, Kobayashi K (2013) Seasonal variations in surface ozone as influenced by Asian summer monsoon and biomass burning in agricultural fields of the northern Yangtze River Delta. Atmos Res 122:67–76. https://doi.org/10.1016/j.atmosres.2012.10.030
65. Tang H, Pang J, Zhang G, Takigawa M, Liu G, Zhu J, Kobayashi K (2014) Mapping ozone risks for rice in China for years 2000 and 2020 with flux-based and exposure-based doses. *Atmospheric Environment*, *86*(2014), 74–83. https://doi.org/10.1016/j.atmosenv.2013.11.078
66. Tran DD, van Halsema G, Hellegers PJGJ, Hoang LP, Ludwig F (2019) Long-term sustainability of the Vietnamese Mekong Delta in question: An economic assessment of water management alternatives. Agric Water Manage 223(June):105703. https://doi.org/10.1016/j.agwat.2019.105703
67. Trieu TTN, Goto D, Yashiro H, Murata R, Sudo K, Tomita H, Satoh M, Nakajima T (2017) Evaluation of summertime surface ozone in Kanto area of Japan using a semi-regional model and observation. Atmos Environ 153:163–181. https://doi.org/10.1016/j.atmosenv.2017.01.030
68. Tu VH, Kopp SW, Trang NT, Hong NB, Yabe M (2021) Land accumulation: An option for improving technical and environmental efficiencies of rice production in the Vietnamese Mekong Delta. Land Use Policy 108(August):105678. https://doi.org/10.1016/j.landusepol.2021.105678
69. Wahid A, Maggs R, Shamsi SRA, Bell JNB, Ashmore MR (1995) Effects of air pollution on rice yield in the Pakistan Punjab. Environ Pollut 90(3):323–329. https://doi.org/10.1016/0269-7491(95)00024-L
70. Wang N, Guo H, Jiang F, Ling ZH, Wang T (2015) Simulation of ozone formation at different elevations in mountainous area of Hong Kong using WRF-CMAQ model. Sci Total Environ 505(x):939–951. https://doi.org/10.1016/j.scitotenv.2014.10.070

71. Wang T, Xue L, Brimblecombe P, Lam YF, Li L, Zhang L (2017) Ozone pollution in China: A review of concentrations, meteorological influences, chemical precursors, and effects. Sci Total Environ 575:1582–1596. https://doi.org/10.1016/j.scitotenv.2016.10.081
72. Wang T, Zhang L, Zhou S, Zhang T, Zhai S, Yang Z, Wang D, Song H (2021) Effects of ground-level ozone pollution on yield and economic losses of winter wheat in Henan, China. Atmos Environ 262(August):118654. https://doi.org/10.1016/j.atmosenv.2021.118654
73. Wassmann R, Phong ND, Tho TQ, Hoanh CT, Khoi NH, Hien NX, Vo TBT, Tuong TP (2019) High-resolution mapping of flood and salinity risks for rice production in the Vietnamese Mekong Delta. Field Crops Research 236(May 2018):111–120. https://doi.org/10.1016/j.fcr.2019.03.007
74. Wilkinson S, Mills G, Illidge R, Davies WJ (2012) How is ozone pollution reducing our food supply? J Exp Bot 63(2):527–536. https://doi.org/10.1093/jxb/err317
75. Xue LK, Wang T, Gao J, Ding AJ, Zhou XH, Blake DR, Wang XF, Saunders SM, Fan SJ, Zuo HC, Zhang QZ, Wang WX (2014) Ground-level ozone in four Chinese cities: Precursors, regional transport and heterogeneous processes. Atmos Chem Phys 14(23):13175–13188. https://doi.org/10.5194/acp-14-13175-2014
76. Yamaguchi M, Hoshino D, Inada H, Akhtar N, Sumioka C, Takeda K, Izuta T (2014) Evaluation of the effects of ozone on yield of Japanese rice (Oryza sativa L.) based on stomatal ozone uptake. Environ Pollut 184:472–480. https://doi.org/10.1016/j.envpol.2013.09.024
77. Zhong Xiaohui, Dutta U (2015) Engaging Nash-Sutcliffe Efficiency and Model Efficiency Factor Indicators in Selecting and Validating Effective Light Rail System Operation and Maintenance Cost Models. J Traffic Transp Eng 3(5):255–265. doi: 10.17265/2328-2142/2015.05.001
78. Zhong Xiaohui and Utpal Dutta, “Engaging Nash-Sutcliffe Efficiency and Model Efficiency Factor Indicators in Selecting and Validating Effective Light Rail System Operation and Maintenance Cost Models,” J. Traffic Transp. Eng., vol. 3, no. 5, pp. 255–265, 2015, doi: 10.17265/2328-2142/2015.05.001.

Figures

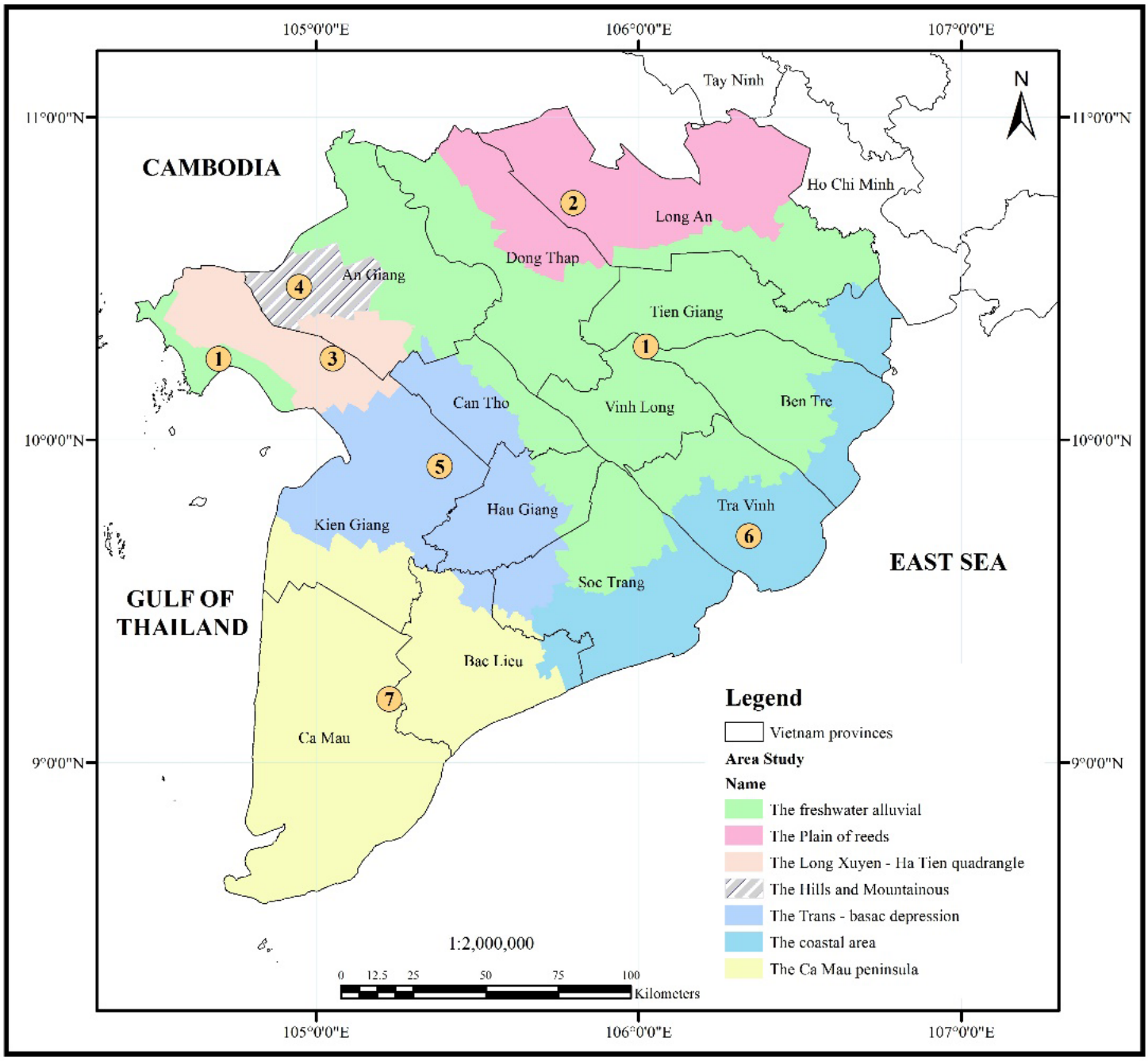

Figure 1

Study area

Figure 2

The measuring sites of ground-level O_3 and meteorological parameters

Figure 3

Implementation steps

Figure 4

Spatio–temporal distribution of average ground-level O_3 concentration in 2018 in the Mekong Delta Region

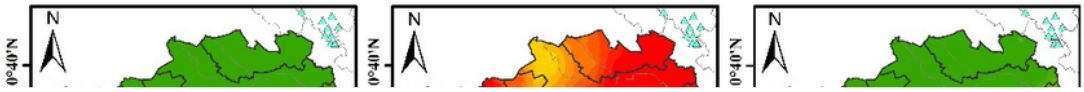

Figure 5

Spatio–temporal distribution of average monthly ground-level O_3 concentrations in the Mekong Delta Region

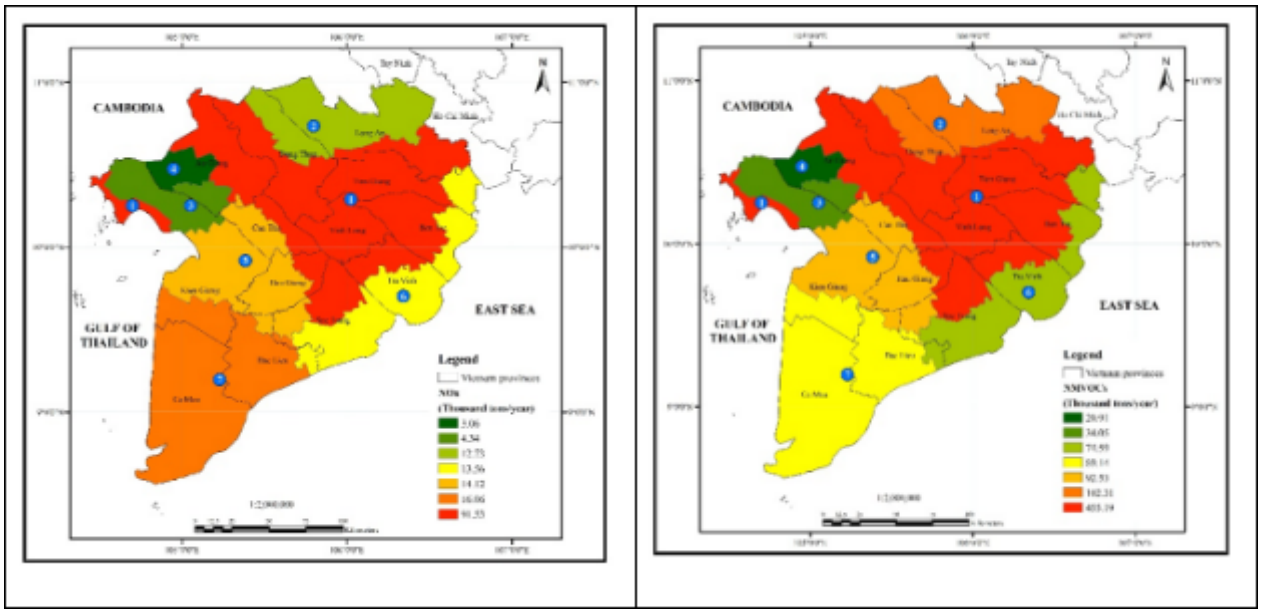

Figure 6

Emission distribution of two precursors NO_x and NMVOCs with major impacts on ozone pollution in the Mekong Delta

Supplementary Files

This is a list of supplementary files associated with this preprint. Click to download.

- AbstractGraphical.jpg
- TableFigureS.docx